Study of the magnetization and magnetic anisotropy of the metal-radical complex of bis(hexafluoroacetylacetonato)manganese(II) with a trisnitroxide radical: $\{Mn(hfac)_2\}_3(3R)_2$

1998 J. Phys.: Condens. Matter 10 2323

(http://iopscience.iop.org/0953-8984/10/10/013)

J. Phys.: Condens. Matter **10** (1998) 2323–2337. Printed in the UK PII: S0953-8984(98)88047-8

Study of the magnetization and magnetic anisotropy of the metal–radical complex of bis(hexafluoroacetylacetonato)manganese(II) with a trisnitroxide radical: $\{Mn(hfac)_2\}_3(3R)_2$

Ashot S Markosyan†§, Takashi Hayamizu‡, Hiizu Iwamura‡ and Katsuya Inoue†

† Applied Molecular Science, Institute for Molecular Science, Nishigounaka 38, Myoudaiji, Okazaki 444, Japan

‡ Institute for Fundamental Research in Organic Chemistry, Kyushu University, Hakozaki 6-10-1, Higashi-ku, Fukuoka 812-81, Japan

Received 30 September 1997

Abstract. A single crystal of the metal–radical complex $\{Mn(hfac)_2\}_3(\mathbf{3R})_2$, where (**3R**) is a trisnitroxide with a quartet ground state, was grown. The magnetization was measured along the principal crystallographic axes in the range 1.8–300 K. The compound was found to order ferrimagnetically at $T_C = 45 \pm 1$ K with collinear antiparallel alignment of the Mn and (**3R**) magnetic spins along the *c*-direction. The paramagnetic susceptibility was treated in the quantum–classical approximation by taking into account the weak positive exchange interaction between the Mn(*2*) ions and one-dimensional ferrimagnetic $\cdots$–Mn(*1*)–(3**R**)–Mn(*1*)–$\cdots$ chains, in which trimer molecules composed of one Mn(*1*) and two 1/2 spins of different triradicals can be isolated. The anisotropy constants were evaluated and the anisotropy energy was estimated. Anisotropy of the paramagnetic susceptibility, which can be detected up to 55 K, was observed. The anisotropic effects are attributed both to the single-ion splitting of the Mn energy levels and the dipole–dipole interaction between the magnetic spins.

1. Introduction

The study of compounds made up of one-dimensional (1D) ferrimagnetic chains is of particular interest in the field of low-dimensional magnetism. Due to a non-zero net magnetization, their behaviour in the ordered state resembles that of three-dimensional (3D) ferro/ferrimagnets, at the same time showing in the paramagnetic state distinctive properties inherent to antiferromagnetic-chain compounds, e.g., a minimum in χT versus T at elevated temperatures (Coronado *et al* 1993). Various bimetallic ferrimagnetic chains have been reported on in the last few years (Pei *et al* 1986a, b, 1987, 1988, Coronado *et al* 1989, 1993). Among these compounds, those containing bimetallic manganese have the strongest magnetic interactions due to the large (5/2) spin of Mn^{2+}, and they often show long-range magnetic order. Since most of the magnetic molecular crystals have low magnetic ordering temperatures, their magnetic anisotropy has been studied mainly by analysing the anisotropy of the magnetic susceptibility (see Carlin (1986) and references therein). Borrãs-Almenar

§ Permanent address: Faculty of Physics, M V Lomonosov Moscow State University, 119899 Moscow, Russia. E-mail: marko@ims.ac.jp/marko@plm.phys.msu.su.

0953-8984/98/102323+15$19.50

et al (1991) pointed out the importance of the single-ion mechanism in the two-sublattice manganese chain compound MnMn(EDTA) $\times$ $9H_2O$ on the basis of measurements of the angular dependence of the ESR spectra. Nevertheless, they mentioned that the single-ion mechanism alone cannot account for the anisotropy of the magnetic susceptibility of this compound and some contribution from the dipole–dipole interaction was also assumed.

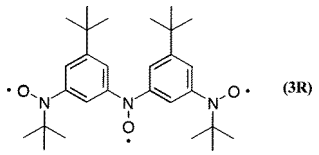

Figure 1. The structure of (**3R**).

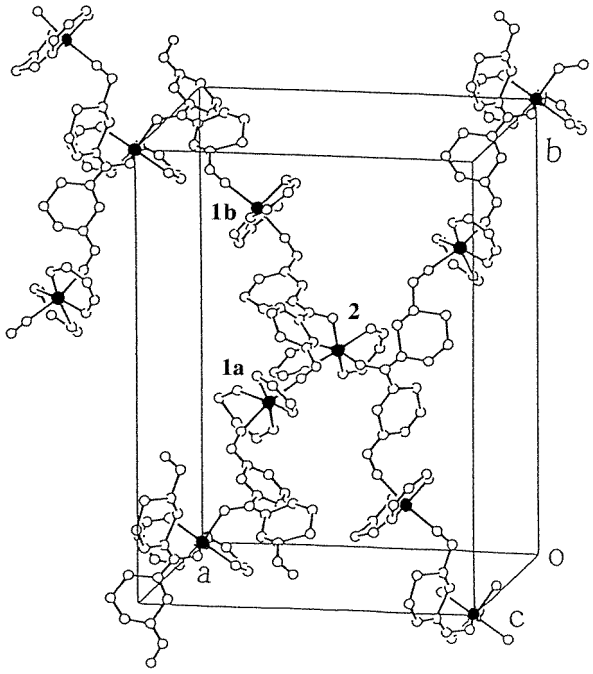

Figure 2. Here we show the crystal structure of the three-dimensional metal–radical complex $\{Mn(hfac)_2\}_3(\mathbf{3R})_2$. The CF_3 and $(CH_3)C$ groups are not shown, for clarity. *a*, *b* and *c* denote the orthorhombic crystal axes. The Mn(*1*) and Mn(*2*) ions are shown by filled circles.

Recently a number of new metal–radical complexes of bivalent Mn^{2+} with bisnitroxide (**2R**) and trisnitroxide (**3R**) were synthesized and characterized (Inoue and Iwamura 1994a, b, Inoue *et al* 1995, Inoue and Iwamura 1996, Inoue *et al* 1996). They show rather versatile magnetic properties depending on the chemical formula and crystal structure. While the $\{Mn(hfac)_2\}$(**2R**) complexes with the biradical (**2R**) form one-dimensional chains and order ferro/ferrimagnetically at low temperatures $\sim$5.5 K (Inoue and Iwamura 1994b, Inoue *et al* 1995), the three-dimensional compound $\{Mn(hfac)_2\}_3(\mathbf{3R})_2$ where (**3R**) is a tris{3-*tert*-butyl-5(T-oxy-*tert*-butylamino)phenyl}nitroxide triradical (see figure 1) has a comparatively high Curie temperature of about 45 K and a high value of the low-temperature spont-

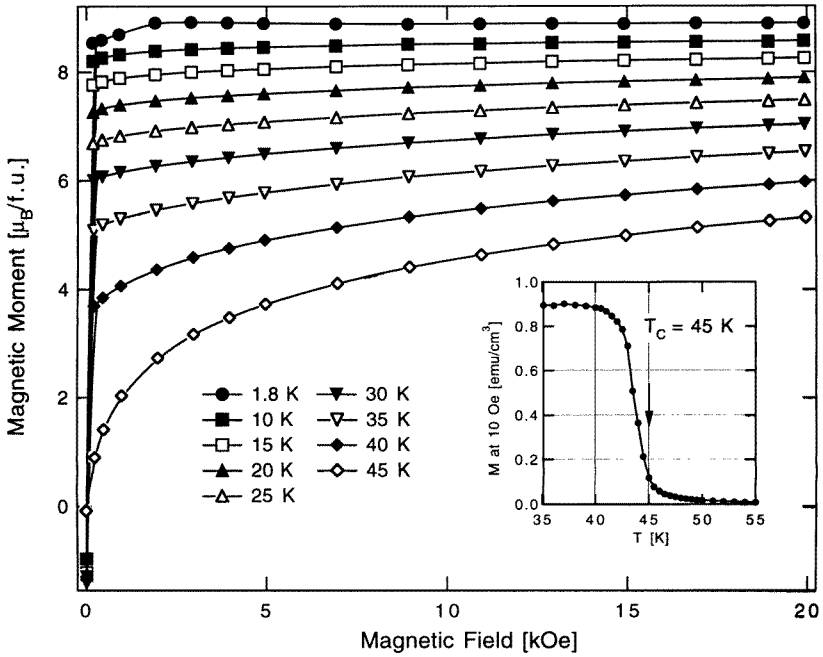

Figure 3. Magnetization curves of the $\{Mn(hfac)_2\}_3(\mathbf{3R})_2$ metal–radical complex at different temperatures. The inset shows the temperature variation of the magnetization at $H = 10$ Oe around T_C.

aneous magnetization M_S (9 μ_B/f.u.) (Inoue *et al* 1996). This complex crystallizes in an orthorhombic system with $Pnn2$ space group and molecular formula $Mn_3F_{36}O_{18}N_6C_{86}H_{90}$ ($Z = 2$). A fragment of its crystal structure is shown in figure 2. The oxygen atoms of the terminal nitroxide group of the triradical (**3R**) are ligated to two manganese ions (*1a* and *1b*) to form a 1D chain in the *bc*-plane of the crystal. Mn ions are attached to two nitroxide oxygens from two different triradical molecules in a *trans*-disposition, so the trisnitroxide molecules are in a zigzag orientation along the chain. The middle nitroxide group of the ligand molecule (**3R**) in the chain is used to link the adjacent chains extended in the $b/-c$ diagonal direction through a third Mn^{2+} ion (*2*). The two nitroxide oxygens are in a *cis*-configuration and the two chains are bridged with the intersecting mean angle of 54.4° establishing a parallel cross-shaped 3D polymeric network.

Magnetization measurements have shown that the $\{Mn(hfac)_2\}_3(\mathbf{3R})_2$ complex has a considerable magnetic anisotropy possibly of a uniaxial type (Inoue and Iwamura 1994b, Inoue *et al* 1995). However, the study of the anisotropic characteristics of $\{Mn(hfac)_2\}_3(\mathbf{3R})_2$ and, in particular, a determination of the anisotropy energy along different crystallographic orientations was not performed in this work. An important problem connected with this complex consists in the determination of the relative strengths of different exchange interactions which specify its temperature-dependent magnetic properties. With the aim of investigating the magnetic properties of $\{Mn(hfac)_2\}_3(\mathbf{3R})_2$, in this work a single crystal of this complex was grown and its magnetization was studied along the three principal axes below and above the Curie temperature. From analysis of these data, the exchange interactions and anisotropy constants were evaluated; different sources contributing to the anisotropy energy are then discussed.

2. Experimental details

The single crystal of the $\{Mn(hfac)_2\}_3(\mathbf{3R})_2$ complex was grown by the evaporation technique in a solution of *n*-heptane, diethyl ether and small amount of chloroform at 0 °C (Inoue *et al* 1996). The crystal structure was measured by using a Rigaku AFC7R diffractometer with graphite-monochromated Mo Kα radiation and a 12 kW rotating anode tube. The lattice parameters were found to take the values $a = 17.82(1)$ Å, $b = 24.367(4)$ Å and $c = 12.522(2)$ Å. The magnetization measurements were performed in a SQUID magnetometer MPMS-7 over the temperature range 1.8–300 K and in fields up to 7 T. The magnetometer was equipped with a rotation mechanism, which allowed us to rotate the single-crystalline sample during the measurements.

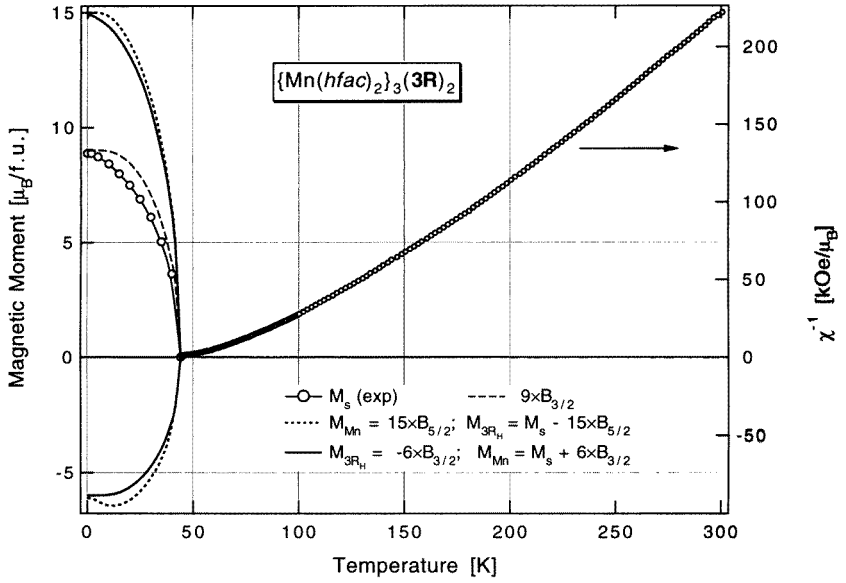

Figure 4. The temperature dependence of the spontaneous and sublattice magnetizations M_S, M_{Mn} and M_{3R} (for the calculated dependences, see the text) and inverse paramagnetic susceptibility of $\{Mn(hfac)_2\}_3(\mathbf{3R})_2$.

3. Experimental data

In figure 3 the magnetic isotherms are shown for the $\{Mn(hfac)_2\}_3(\mathbf{3R})_2$ complex at different temperatures in the magnetically ordered region measured along the easy axis *c*. They are characterized by very narrow hysteresis and a monotonic decrease of the saturation magnetization. The low-temperature value of the saturation magnetization, 8.9 μ_B/f.u., corresponds well to a collinear ferrimagnetic structure if one takes $\mu_{Mn} = 5\ \mu_B$ and $\mu_{3R} = 3\ \mu_B$. This confirms the spin states of Mn^{2+} (5/2) and trisnitroxide (3/2) established earlier (Inoue *et al* 1996) as well as the collinear ferrimagnetic structure of $\{Mn(hfac)_2\}_3(\mathbf{3R})_2$. The temperature dependence of the magnetization traced at a constant field of 10 Oe changes sharply at 45 ± 1 K (see the inset in figure 3), which was identified as the Curie temperature.

In figure 4 we show the temperature dependence of the spontaneous magnetization, M_S,

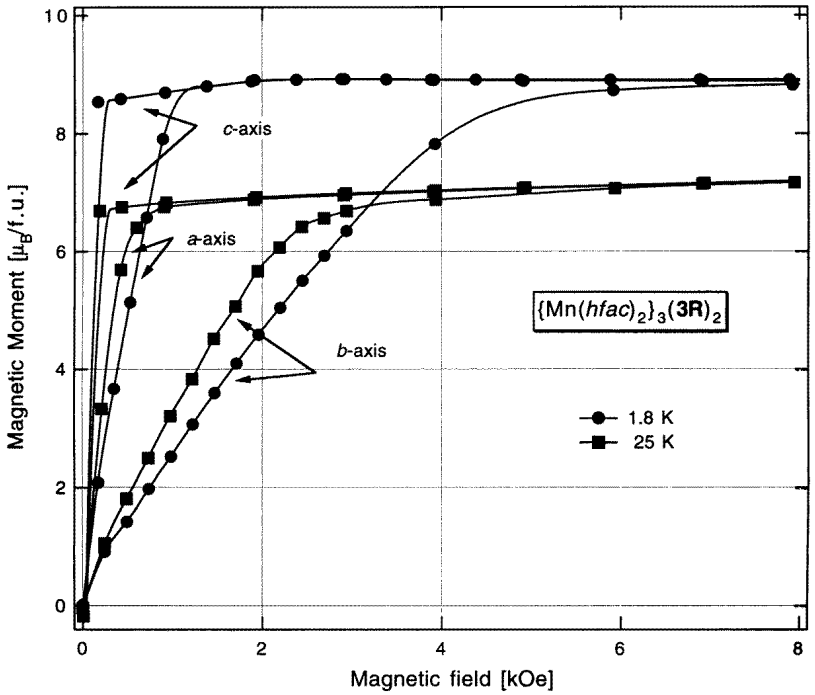

Figure 5. Magnetization curves of $\{Mn(hfac)_2\}_3(\mathbf{3R})_2$ at 1.8 and 25 K along the three principal crystallographic axes.

of $\{Mn(hfac)_2\}_3(\mathbf{3R})_2$. The values of M_S evaluated from the measurements along different axes were equal to each other, i.e. no anisotropy of the saturation magnetization is observed. As can be seen, M_S falls monotonically with increasing temperature. This dependence does not follow the Brillouin function $B_{3/2}$ expected for simple 3D ferromagnets if one assumes each Mn^{2+} ion to be antiferromagnetically coupled with the two 1/2 spins of different triradicals to form basic molecular species with $S = 3/2$. In fact, M_S falls even faster than $B_{5/2}(T)$.

Within the range of application of the 3D approximation for the magnetic interactions, it is also possible to consider the net magnetization as a difference between the Mn and (**3R**) radical sublattice magnetizations, $M_S(T) = M_{Mn}(T) - M_{\mathbf{3R}}(T)$. Assuming that the temperature dependence of the Mn-sublattice magnetization follows the Brillouin function $B_{5/2}(T)$, the sublattice magnetization of the nitroxide triradical species can be written as $M_{\mathbf{3R}}(T) = |M_S(T) - 15B_{5/2}(T/T_C)|$, where T_C is taken as 45 K. The temperature variation of M_{3R} evaluated by using this equation is depicted in figure 4 together with the Brillouin function $B_{5/2}(T)$ normalized to 15 μ_B used for the Mn sublattice (dotted lines). The magnetization of the (**3R**) sublattice thus obtained increases with the temperature increasing from 1.8 K and passes over a maximum (6.4 μ_B) at 15 K. This is inconsistent with the low-temperature value 6 μ_B. The next simple approach, using $B_{3/2}$ for the temperature dependence of the (**3R**)-sublattice magnetization, gives a monotonic temperature variation for $M_{Mn}(T)$, although distinct from $B_{5/2}$ (solid lines in figure 4).

The temperature dependence of the inverse susceptibility, χ^{-1}, of $\{Mn(hfac)_2\}_3(\mathbf{3R})_2$ shown in figure 4 varies non-linearly up to the highest temperature measured, i.e. does not follow the Curie law, and neither does it show the negative curvature expected for 3D

ferrimagnets (the Néel law).

In figure 5 the magnetization curves along the three principal crystallographic axes are presented for the $\{Mn(hfac)_2\}_3(\mathbf{3R})_2$ complex. As can be seen, the *b*-axis is the hard direction of magnetization, and the *a*-axis corresponds accordingly to the intermediate direction. This hierarchy is retained up to the Curie temperature.

4. Discussion

4.1. Determination of exchange interactions

The exchange interactions determining the isotropic magnetic properties of the $\{Mn(hfac)_2\}_3(\mathbf{3R})_2$ compound were evaluated from analysis of the temperature dependence of the paramagnetic susceptibility. All of the attempts to describe this dependence within the framework of 3D ferromagnetic or ferrimagnetic models by combining different magnetic sublattices made up either from Mn^{2+} and (**3R**) molecules or ($\bar{1}/2$, $5/2$, $\bar{1}/2$) species formed by Mn^{2+} and nitroxide groups were unsuccessful. This accounted for the effect of a magnetic low dimensionality that the $\{Mn(hfac)_2\}_3(\mathbf{3R})_2$ compound exhibits at least in the paramagnetic region. Although this complex forms a well defined three-dimensional network with respect to the chemical bondings, the spin–spin couplings between Mn^{2+} and triradical species can be different along different directions, which can in turn modify the paramagnetic behaviour of $\chi(T)$ substantially in the temperature range below 300 K.

The paramagnetic susceptibility of $\{Mn(hfac)_2\}_3(\mathbf{3R})_2$ was examined by using a model in which the triradicals were assumed to form 1D ferrimagnetic chains with the Mn(*1*) ions in the positions *1a* and *1b* (figure 2), while the Mn(*2*) ions in positions *2* link them through the exchange interaction with the middle nitroxide group of (**3R**). This assumption means that the exchange interaction between Mn(*1*) and the terminal nitroxide group is substantially stronger than the interaction between Mn(*2*) and the middle nitroxide group of (**3R**). A similar chain compound, equimolar $\{Mn(hfac)_2\}(\mathbf{3R})$, made up of bivalent manganese and nitroxide triradicals is known to show a magnetic one dimensionality (Inoue *et al* 1995).

In fact, the $\{Mn(hfac)_2\}_3(\mathbf{3R})_2$ complex is not a true 1D-chain compound because the magnetic contribution of the Mn(*2*) ions linking the $\cdots$ –Mn(*1*)–(**3R**)–Mn(*1*)– $\cdots$ chains can be neither neglected nor considered as a kind of paramagnetic impurity. Moreover, the 1D chains themselves have a four-spin periodicity which prevents one from performing any exhaustive analysis by the use of existing analytical expressions derived for ferrimagnetic chains with two-spin periodicity (Seiden 1983, Drillon *et al* 1983, Verdaguer *et al* 1984, Pei *et al* 1988, Qiang Xu *et al* 1988, Coronado *et al* 1989). Therefore the approach applied to interpret the paramagnetic susceptibility of $\{Mn(hfac)_2\}_3(\mathbf{3R})_2$ contains some simplifications. The complex $\{Mn(hfac)_2\}_3(\mathbf{3R})_2$ was on the whole considered as a two-sublattice ferrimagnet formed by isolated Mn(*2*) ions and $\cdots$ –Mn(*1*)–(**3R**)–Mn(*1*)– $\cdots$ chains with a positive intersublattice exchange interaction. Then, in the molecular-field approximation the low-field paramagnetic susceptibility of this compound can be written in the conventional form

$$\chi_{\mathrm{tot}} = \frac{(C_{\mathrm{Mn}} + C_{\mathrm{ch}})T + C_{\mathrm{Mn}}C_{\mathrm{ch}}(2\lambda' - \lambda_{\mathrm{Mn}} - \lambda_{\mathrm{ch}})}{T^2 - (C_{\mathrm{Mn}}\lambda_{\mathrm{Mn}} + C_{\mathrm{ch}}\lambda_{\mathrm{ch}})T - C_{\mathrm{Mn}}C_{\mathrm{ch}}[(\lambda')^2 - \lambda_{\mathrm{Mn}}\lambda_{\mathrm{ch}}]} \qquad (1)$$

where λ' is the intersublattice molecular-field coefficient, λ_{Mn} and λ_{ch} are the intrasublattice

molecular-field coefficients for the Mn(*2*) and 1D-chain sublattices and

$$C_{\mathrm{Mn}} = N\frac{g^2\mu_{\mathrm{B}}^2}{3k}S_{\mathrm{Mn}}(S_{\mathrm{Mn}}+1) \qquad C_{\mathrm{ch}} = \chi_{\mathrm{ch}}T \tag{2}$$

are accordingly the Curie constants of the Mn(*2*) and chain sublattices. In equations (1) and (2) the intrachain exchange interaction is included in C_{ch}, which is hence a temperature-dependent quantity described as 'constant' for convenience only.

In order to calculate the temperature dependence of $\chi_{\mathrm{ch}}T$, the $\cdots$–Mn(*1*)–(**3R**)–Mn(*1*)–$\cdots$ chain was approximated by a model in which molecular species having stable spins in the temperature region up to 300 K were isolated. According to the chain structure, two possible configurations were considered:

(i) a ferrimagnetic (*5/2–3/2*) chain formed of nitroxide radicals (**3R**) with $S_{\mathrm{R}} = 3/2$ antiferromagnetically coupled with Mn(*1*); and

(ii) a ferrimagnetic (*3/2–1/2*) chain formed of the trimeric spin species made up of one Mn(*1*) ion and two terminal nitroxide groups of different triradicals ($S_{\mathrm{TR}} = 3/2$) antiferromagnetically coupled with the middle nitroxide group spin ($s = 1/2$).

For the tentative analysis, the chain susceptibility was considered in the Heisenberg classical–classical spin approximation by using the expression (Coronado *et al* 1989)

$$(\chi_{\mathrm{ch}}T)_{\mathrm{classical}} = \frac{N\mu_{\mathrm{B}}^2}{3k}\left(g_+^2\frac{1+U}{1-U} + g_-^2\frac{1-U}{1+U}\right) \tag{3}$$

where the following notation is used (all of the exchange interactions are represented in this work in the form $-2JS_iS_j$):

$$K = \coth\frac{T_0}{T} - \frac{T}{T_0}$$

$$T_0 = \left(\frac{2J_{\mathrm{ch}}}{k}\right)\sqrt{S_1(S_1+1)S_2(S_2+1)}$$

$$g_\pm = \frac{1}{2}(g_1 \pm g_2) \qquad g_i = 2\sqrt{S_i(S_i+1)} \qquad (i = 1, 2)$$

all of the other symbols having their usual meaning. Note that here J_{ch} is an effective parameter for describing the intrachain Mn(*1*)–(**3R**) negative exchange and will not be considered as an exchange integral.

The least-squares fitting procedure used to fit equation (1) to the experimental data by the use of the complete set of parameters λ', λ_{Mn}, λ_{ch} and $2J_{\mathrm{ch}}/k$ is rather questionable. Therefore, the intrasublattice exchange interactions were set to zero for the preliminary fits. This assumption is plausible since no exchange paths can be found for the Mn(*2*)–Mn(*2*) and chain–chain interactions. Then the stability of the solutions was checked by letting λ_{Mn} and λ_{ch} vary freely. For the (*5/2–3/2*) spin configuration no satisfactory fitting was possible with negative values of $2J_{\mathrm{ch}}/k$ and positive λ'-values. In contrast, the (*3/2–1/2*) configuration gives a good fit for $\chi_{\mathrm{tot}}T$ over a rather wide temperature range, 70–300 K, with reasonable values of $2J_{\mathrm{ch}}/k$ and λ', and $\lambda_{\mathrm{Mn}} \approx \lambda_{\mathrm{ch}} = 0 \pm 0.5$ K. The results obtained on applying this procedure are listed in table 1.

The determination of the exchange interaction parameters for the (*3/1–1/2*) configuration was finally carried out in the quantum–classical chain approximation by using the analytical expression for the paramagnetic susceptibility of a ferrimagnetic chain derived by Seiden

Table 1. Exchange parameters of {Mn(*hfac*)$_2$}$_3$(**3R**)$_2$ and {M*n*(*hfac*)$_2$}(**3R**): the numbers of nearest neighbours for the intersublattice exchange interaction $2J'/k$ are taken as 2 and 6, respectively.

Model	$2J_{ch}/k$ (K)	λ' (emu mol^{-1})	$2J'/k$ (K)	J_{Tr}/k (K)
{Mn(*hfac*)$_2$}$_3$(**3R**)$_2$				
Classical–classical	-900 ± 30	$+5.9 \pm 0.4$	$+4.4$	$S_{Tr} = 3/2$
Quantum–classical	-520 ± 20	$+5.2 \pm 0.4$	$+3.9$	$S_{Tr} = 3/2$
Quantum–classical	-520 ± 20	$+5.1 \pm 0.4$	$+3.8$	$\leqslant -350$
{Mn(*hfac*)$_2$}(**3R**)				
Quantum–classical	-80 ± 10	0	0	-135 ± 15
Quantum–classical	-100 ± 10	-2.6 ± 0.3	-0.65	-120 ± 15

(1983) (see also Coronado *et al* 1993):

$$(\chi_{ch}T)_{Qu} = \frac{N\mu_B^2}{3k}\left\{S_{TR}(S_{TR}+1) + \frac{3}{4} + \frac{2}{1-P(\gamma)}[S_{TR}(S_{TR}+1)P(\gamma) - S_{TR}Q(\gamma) + 0.25Q^2(\gamma)]\right\}. \quad (4)$$

Here $\gamma = -2J_{ch}S_{TR}/kT$ and

$$P(\gamma) = \frac{(1+12\gamma^{-2})\sinh\gamma - (5\gamma^{-1}+12\gamma^{-3})\cosh\gamma - \gamma^{-1} + 12\gamma^{-3}}{\sinh\gamma - \gamma^{-1}\cosh\gamma + \gamma^{-1}}$$

$$Q(\gamma) = \frac{(1+2\gamma^{-2})\cosh\gamma - 2\gamma^{-1}\sinh\gamma - 2\gamma^{-2}}{\sinh\gamma - \gamma^{-1}\cosh\gamma + \gamma^{-1}}.$$

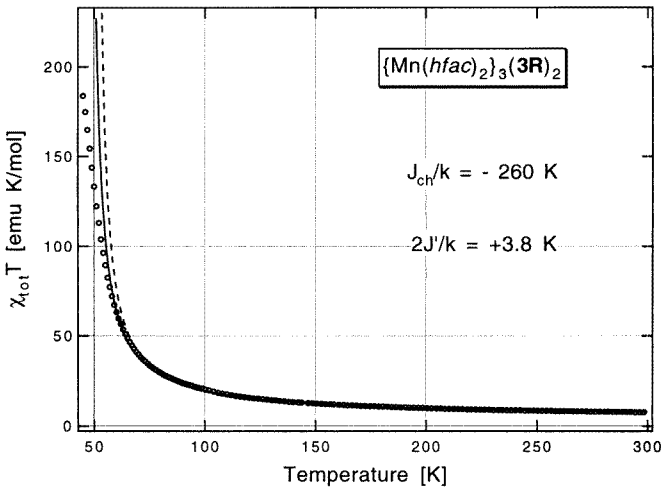

Figure 6. The temperature dependence of the product $\chi_{tot}T$ of the {Mn(*hfac*)$_2$}$_3$(**3R**)$_2$ complex in the paramagnetic temperature range. Open circles show the experimental data; the solid and dashed lines were calculated for the fixed trimer spin $S_{Tr} = 3/2$ in the quantum–classical and classical–classical approximations, respectively.

The best fits were found near the zero values for λ_{Mn} and λ_{ch} and the final fit was again made with two variables. In figure 6 the calculated and experimental temperature dependences of $\chi_{tot}T$ for $\{Mn(hfac)_2\}_3(\mathbf{3R})_2$ are compared. They are in good agreement over a wide temperature range down to about 55 K. The parameters corresponding to this procedure are given in table 1, too. The difference observed between the classical–classical and quantum–classical approaches is not surprising. According to the calculations of Coronado *et al* (1989), the solutions for the two models start to differ below $T \approx 2|J_{ch}|/k$, i.e. for $\{Mn(hfac)_2\}_3(\mathbf{3R})_2$ below about 250 K.

The results obtained show that the $\{Mn(hfac)_2\}_3(\mathbf{3R})_2$ complex is characterized by very strong intrachain interactions. The possibility of isolating trimeric spin species ($\bar{1}/2$, $5/2$, $\bar{1}/2$) in the $\cdots$–Mn(*1*)–(**3R**)–Mn(*1*)–$\cdots$ chain indicates that the exchange interaction between Mn(*1*) and the terminal nitroxide group substantially exceeds the interaction energy between the NO groups within the (**3R**) radical, which is characterized by the exchange integral $2J/k = +480$ K (Ishida and Iwamura 1991).

4.2. The effect of intratrimer interaction

Due to the strong intratrimer exchange interaction, the model with a fixed S_{TR}-value appears to be applicable over the temperature range up to 300 K. However, this approach will fail at temperatures higher than the intratrimer interaction parameter J_{Tr}/k. In order to reveal the role of the intratrimer interaction in the temperature dependence of $\chi_{tot}T$, a fitting procedure was carried out with S_T replaced by the effective moment of the ($\bar{1}/2$, $5/2$, $\bar{1}/2$) trimer:

$$\mu_{Tr}^2 = \frac{3k}{Ng^2\mu_B^2}(\chi_{Tr}T)$$

in equation (4). The exchange interactions in this trimer can be described by the isotropic spin Hamiltonian $H = -2J_{Tr}(\boldsymbol{s}_1 \cdot \boldsymbol{S}_2 + \boldsymbol{S}_2 \cdot \boldsymbol{s}_3)$. The eigenvalues $E(S_T, S_{13})$ of this Hamiltonian are $E(3/2, 1) = 7J_{Tr}$, $E(5/2, 1) = 2J_{Tr}$, $E(5/2, 0) = 0$ and $E(7/2, 1) = -5J_{Tr}$ (where $S_T = S_2 + S_{13}$ and $S_{13} = s_1 + s_{13}$). From these energies the equation for the molar susceptibility of the trimer molecule ($\bar{1}/2$, $5/2$, $\bar{1}/2$) was found:

$$\chi_{Tr} = N\frac{g^2\mu_B^2}{4kT}\left(5 + 4\frac{16 + 5e^{-5J_{Tr}/kT} + 5e^{-7J_{Tr}/kT}}{4 + 3e^{-5J_{Tr}/kT} + 3e^{-7J_{Tr}/kT} + 2e^{-12J_{Tr}/kT}}\right) \qquad (5)$$

and a fit of equation (1) to the experimental data was made. The temperature variation of $\chi_{tot}T$ for the $\{Mn(hfac)_2\}_3(\mathbf{3R})_2$ complex appeared to be unaffected by the intratrimer exchange interaction. In fact, a change of the fit parameters lies within the accuracy of the procedure (see table 1). Hence, $|J_{Tr}|/k$ was estimated to be larger than 350 K.

In figure 7 the temperature dependences of $\chi_{tot}T$ calculated for $\{Mn(hfac)_2\}_3(\mathbf{3R})_2$ by using different sets of the exchange parameters are extrapolated into the high-temperature region. As can be seen, the presence of the Mn(*2*) ferromagnetic sublattice does not eliminate the minimum in $\chi_{tot}T$ expected for conventional 1D ferrimagnetic- or antiferromagnetic-chain compounds. In contrast, the population of the excited states of the trimer makes the minimum in $\chi_{tot}T$, which is predicted to lie at about 500 K, more pronounced as compared to the case of a stable biperiodical ferrimagnetic chain. The inset in figure 7 shows the temperature dependence of μ_{Tr}^2 calculated for the ($\bar{1}/2$, $5/2$, $\bar{1}/2$) trimer. The most prominent change of the effective moment occurs in the temperature range $1.5 < kT/|J_{Tr}| < 5$. In this range the effect of trimerization must be the most significant.

The 1D-chain compound $\{Mn(hfac)_2\}(\mathbf{3R})$ is an appropriate object for applying the above approach to in order to display the effect of trimerization. In this compound, the 1D chains made up of Mn^{2+} and triradicals (**3R**) are directly linked with each other by

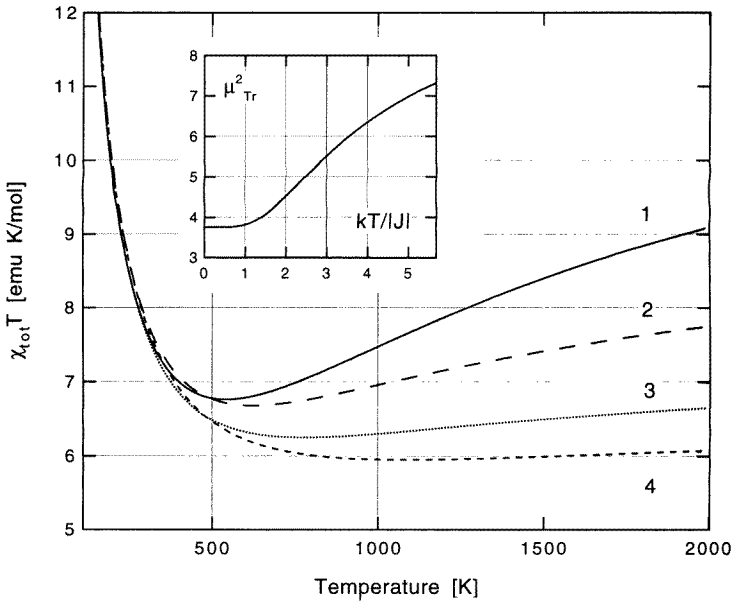

Figure 7. Here we show the high-temperature extrapolation of $\chi_{tot}T$ versus temperature for the {Mn(*hfac*)$_2$}$_3$(**3R**)$_2$ complex calculated in different approximations for $\chi_{ch}T$: quantum–classical, $J_{Tr}/k = -350$ K (1); classical–classical, $J_{Tr}/k = -350$ K (2); quantum–classical, $S_{Tr} = 3/2$ (3); and classical–classical, $S_{Tr} = 3/2$ (4). The inset shows the temperature dependence of μ^2_{Tr} calculated for the ($\bar{1}/2$, *5/2*, $\bar{1}/2$) configuration by the use of equation (5).

nitroxide groups (Inoue *et al* 1995). It crystallizes in the monoclinic $P2_1/c$ structure with $a = 10.137(3)$ Å, $b = 19.426(5)$ Å, $c = 27.187(7)$Å and $\beta = 95.21(2)^\circ$. Below $T_N = 11$ K a transition into a 3D antiferromagnetic state occurs in this compound. The high-field magnetization value 2 μ_B/f.u. indicates that the Mn^{2+} ($S = 5/2$) and (**3R**) ($S = 3/2$) moments within the chains are aligned antiparallel. In figure 7 the temperature dependence of χT for {Mn(*hfac*)$_2$}(**3R**) is given. At $T_{min} = 115$ K the dependence shows a pronounced characteristic minimum. Any attempts to fit equation (4) to the experimental curve by using either (*5/2–3/2*) or (*3/2–1/2*) stable configurations were unsuccessful: fits cannot be made either above or below T_{min}.

Considering two different possibilities for trimerization, *5/2*–(*1/2*, *1/2*, *1/2*)–*5/2* and *1/2*–($\bar{1}/2$, *5/2*, $\bar{1}/2$)–*1/2*, the latter configuration was found to describe quite well the experimental data. The dashed line in figure 8 corresponds to the fitting procedure which neglects the weak interchain interaction. It describes satisfactorily the experimental curve both above and below T_{min}. By introducing the interchain exchange parameter λ', the agreement can be substantially improved (the solid line in figure 8). The result of a three-parameter fitting, although it cannot be considered as being unambiguously quantitative, shows that the low-temperature behaviour of χT obeys the above model as well. The exchange parameters of {Mn(*hfac*)$_2$}(**3R**) are also listed in table 1.

Several factors can give rise to the difference in the strength of the intratrimer and intrachain interactions found between {Mn(*hfac*)$_2$}$_3$(**3R**)$_2$ and {Mn(*hfac*)$_2$}(**3R**). The difference in the Mn(*1*)–O–N angles seems not to be dominant, as it favours more the latter compound to have stronger exchange interactions. This will probably be of importance for ions with $L \neq 0$. In {Mn(*hfac*)$_2$}$_3$(**3R**)$_2$ the Mn(*1*)–O distances are however slightly shorter

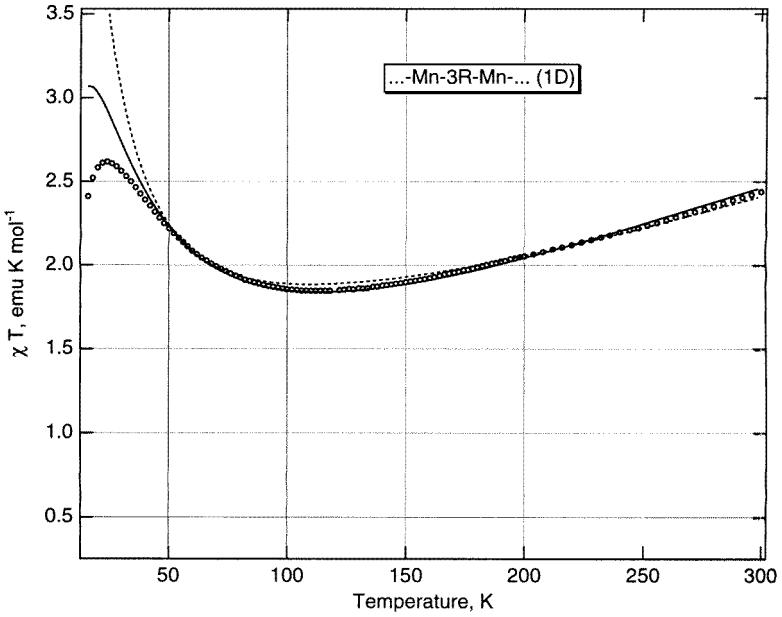

Figure 8. The temperature variation of the product $\chi_{tot}T$ for the equimolar $\{Mn(hfac)_2\}(\mathbf{3R})$ complex in the paramagnetic temperature range. Open circles show the experimental data. The solid and dashed lines show the temperature dependences calculated by taking into account the effect of trimerization (respectively with and without interchain exchange interaction).

than in $\{Mn(hfac)_2\}(\mathbf{3R})$: 2.10(1) Å versus 2.14(1) Å. This is an isotropic mechanism, which might be considered as being responsible for the observed regularity.

4.3. Determination of the anisotropy constants

The magnetic anisotropy of $\{Mn(hfac)_2\}_3(\mathbf{3R})_2$ appears to be not very high compared to those of the other, metallic as well as non-metallic, magnetic compounds with zero 3d orbital moments. A rough estimate, made on the basis of the area lying between the magnetization curves along the easy and hard axes, shows that the energy associated with the anisotropy, E_A, is more than one order of magnitude less than the total magnetic energy. Hence, E_A can be expressed through the phenomenological anisotropy constants K_n^m by expansion into a series in the polar (θ) and azimuthal (ϕ) coordinate angles of the magnetization vector $\boldsymbol{M}$ (Franse and Radwanski 1993):

$$E_A = \sum_{n=0}^{\infty}\sum_{m=0}^{n} K_n^m \sin^n\theta\cos m\phi.$$

The number of the non-zero terms is limited by symmetry. For the case of orthorhombic crystals the anisotropy energy takes the form

$$E_A = K_1\sin^2\theta + K_2\sin^4\theta + \cdots + K_1'\sin^2\theta\cos 2\phi + K_2'\sin^4\theta\cos 2\phi + \cdots \tag{6}$$

and must therefore be described in the second approximation using four anisotropy constants.

The angular dependence of E_A can hence be calculated if the values of K_i are known. The maximal anisotropy energy corresponding to the difference between the magnetization processes along the easy and hard axes is in this notation $E_{eh} = K_1 + K_2 - K_1' - K_2'$.

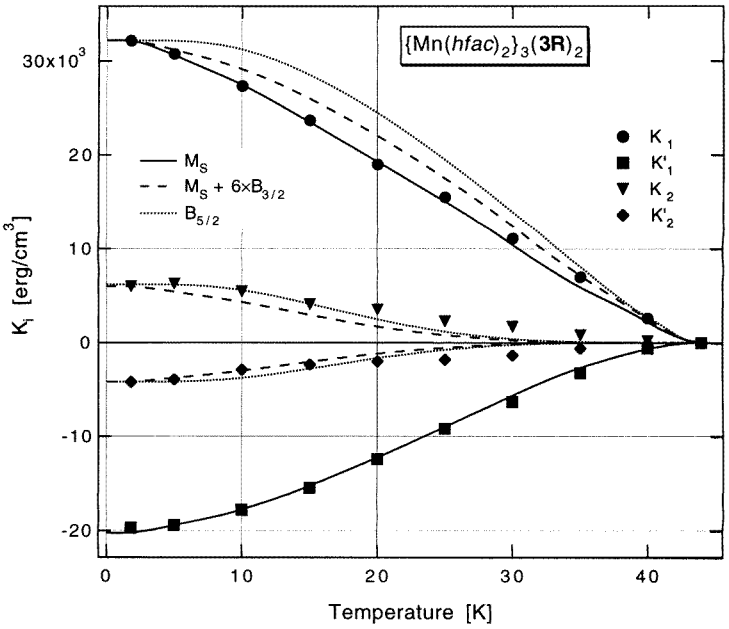

Figure 9. The temperature dependence of the anisotropy constants of $\{Mn(hfac)_2\}_3(\mathbf{3R})_2$. Dotted and dashed lines correspond to the temperature dependences approximated as M^3_{Mn} (K_1) and M^{10}_{Mn} (K_2 and K'_2) and normalized to 0 K, and the solid lines for K_1 and K'_1 are normalized $M^3_S(T)$ dependencies (for details, see the text).

In this work, the anisotropy constants of $\{Mn(hfac)_2\}_3(\mathbf{3R})_2$ were determined in terms of the Sucksmith–Thompson method by analysing H/M versus M^2 plots along the intermediate ($\phi = 0$) and hard ($\phi = \pi/2$) directions (Sucksmith and Thompson 1954). These plots were found to vary linearly in the field region $H < H_A$ (H_A is the anisotropy field) with non-zero slopes with respect to the M^2 coordinate axis, indicating that the terms of higher order than $\sin^4\theta$ in equation (6) are negligible. In figure 9 the temperature dependences of K_i for the $\{Mn(hfac)_2\}_3(\mathbf{3R})_2$ complex are presented. They decrease monotonically with increasing temperature without any changes in sign. The numerical values of the anisotropy constants at the lowest temperature measured, 1.8 K, are $K_1 = +3.2 \times 10^4$ erg cm^{-3}, $K'_1 = -2.0 \times 10^4$ erg cm^{-3}, $K_2 = +6.0 \times 10^3$ erg cm^{-3} and $K'_2 = -4.2 \times 10^3$ erg cm^{-3}.

Several sources can contribute to the anisotropy of magnetic crystals. All of the models relate the temperature dependence of K_i to that of the spontaneous magnetization. Numerous data on different Mn^{2+}-based compounds and radical complexes show that the Heisenberg model dealing with isotropic exchange interactions describes well the magnetic behaviour of these compounds (Carlin 1986). Hence, anisotropy of the exchange interaction seems to be unimportant in the $\{Mn(hfac)_2\}_3(\mathbf{3R})_2$ complex. In the magnetic compounds containing atoms with a non-zero orbital magnetic moment, the crystallographic magnetic anisotropy is considered to be caused by the single-ion mechanism. The source of this anisotropy is the interaction of the non-spherical 3d, 4f or 5f electronic shells with the crystal electric field via the spin–orbit coupling. The value of the anisotropy energy reaches 10^7–10^8 erg cm^{-3} in f compounds and usually is substantially smaller (10^6–10^7 erg cm^{-3}) in those based on 3d elements (see, e.g., Franse and Radwanski 1993). The compounds with S ions, Fe^{3+}, Mn^{2+} and Gd^{3+}, with spherical magnetic electronic shells exhibit substantially lower anisotropy,

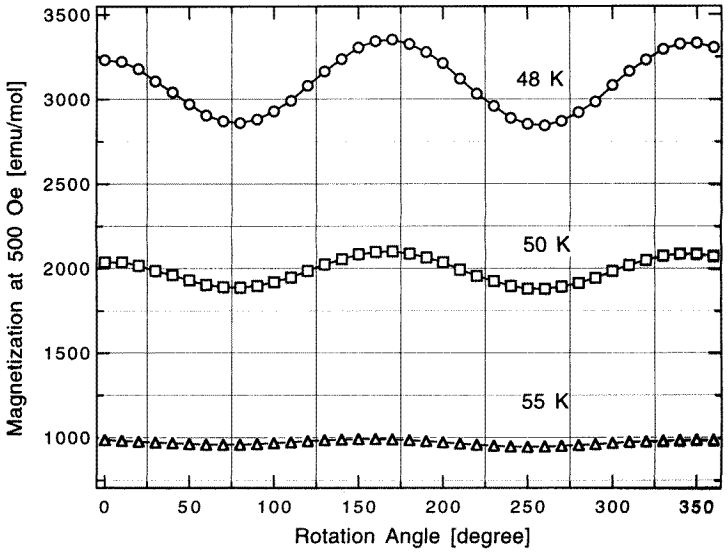

Figure 10. The angular dependence of the low-field magnetization of $\{Mn(hfac)_2\}_3(\mathbf{3R})_2$ at different temperatures in the paramagnetic region measured in the (ac) crystallographic plane.

as in the first approximation the crystal field does not influence the orientation of their atomic magnetic moments.

In the case of Mn^{2+}, the single-ion contribution appears in the second-order perturbation theory only and should therefore be small. This hinders the analysis of magnetic anisotropy in S-ion compounds since different mechanisms contributing to the anisotropy energy become comparable and cannot be separated easily. In the circumstances, the magnetic dipole–dipole interaction either between the Mn^{2+} spins or between the Mn^{2+} and (**3R**) spins is a factor which cannot be neglected when considering the magnetic anisotropy of $\{Mn(hfac)_2\}_3(\mathbf{3R})_2$. Bivalent manganese has the highest spin moment, 5/2, among the 3d transition elements, which favours a large strength of the dipole–dipole interaction.

Some conclusions about the nature of the magnetic anisotropy of $\{Mn(hfac)_2\}_3(\mathbf{3R})_2$ can be reached by considering the temperature dependence of the anisotropy constants. In crystals with uniaxial anisotropy, the single-ion mechanism predicts a low-temperature variation of K_i proportional to M^3 (for $i = 1$) and M^{10} (for $i = 2$). Assuming that the observed magnetic anisotropy is mainly associated with the Mn sublattice, in figure 9 the temperature dependence of the anisotropy constant K_1 is compared with $M^3_{Mn}(T)$ where both $M_S + 6B_{3/2}$ (dashed line) and $B_{5/2}$ (dotted line) are used as M_{Mn}. As can be seen, the curves do not match the experimental one. The same holds for K_1'. Note, however, that at low temperatures the second-order anisotropy constants can be approximated satisfactorily by the $M^{10}_{Mn}(T)$ dependencies in accordance with the single-ion mechanism.

The temperature variation of the first-order constants is well approximated by $M^3_S(T)$, the third power of the net magnetization. This fact shows that the Mn contribution alone cannot explain the observed magnetic anisotropy of $\{Mn(hfac)_2\}_3(\mathbf{3R})_2$, if we are to remain within the scope of the single-ion model. The anisotropic term of the dipole–dipole interaction for collinear alignment of the magnetic moments μ_i and μ_j can be written as

$$E_{DA} = \left(\sum_{i \neq j} \frac{\mu_i \mu_j}{R^3_{ij}}\right) \sin^2 \psi \tag{7}$$

where the R_{ij} are the interatomic distances and ψ is the angle that μ_i and μ_j make with R_{ij}. Following equation (7), the second-order constants K_2 and K_2' must be equal to zero in $\{Mn(hfac)_2\}_3(\mathbf{3R})_2$. This is an important argument for accepting the existence of a single-ion contribution to the magnetic anisotropy of $\{Mn(hfac)_2\}_3(\mathbf{3R})_2$. An exact calculation of the dipole–dipole interaction in this compound cannot easily be made, since the spin density of the radical is spatially substantially delocalized. Nevertheless, the anisotropy energy $\Delta E_{eh} = 6.2 \times 10^4$ erg cm^{-3} $\approx 5.6 \times 10^{-17}$ erg/Mn ion observed for $\{Mn(hfac)_2\}_3(\mathbf{3R})_2$ at 1.8 K is of the same order of magnitude as that for other Mn compounds where the dipole–dipole interaction was taken into consideration in order to explain the magnetic anisotropy (Carlin 1986, Wonsowski 1971). The situation with $\{Mn(hfac)_2\}_3(\mathbf{3R})_2$ has some similarity with that for the chain compound MnMn(EDTA) $\times$ $9H_2O$ (Borrãs-Almenar *et al* 1991) in which both of the mechanisms were found to be of importance. As for MnMn(EDTA) $\times$ $9H_2O$, Mn ions in $\{Mn(hfac)_2\}_3(\mathbf{3R})_2$ occupy two inequivalent positions with different local symmetries and can therefore give different contributions to the dipole–dipole and single-ion anisotropy energies.

Finally, we note that in spite of the apparently simple behaviour of the anisotropic characteristics, some properties of $\{Mn(hfac)_2\}_3(\mathbf{3R})_2$ require investigation in more detail. This concerns, in particular, the anisotropy of the paramagnetic susceptibility. As can be seen from figure 10, where the angular dependence of the magnetization at 500 Oe in the (ac) crystallographic plane is presented, a considerable difference exists above T_C. The ratio $\Delta\chi/\chi = (\chi_{easy} - \chi_{intermediate})/\chi_{easy} \approx 18\%$ at 48 K drops rapidly with increasing temperature (12% at 50 K) and can hardly be detected above 60 K. Although this anisotropy can also be attributed to the dipole–dipole interaction as was concluded for some other compounds containing bivalent manganese, e.g. $(CH_3)_4NMnCl_3$ (Walker *et al* 1972), detailed calculations are desirable in order to ascertain whether the single-ion splitting of the Mn levels can give rise to this anisotropy.

5. Conclusions

The magnetic properties of the ferrimagnetic three-dimensional metal–radical complex $\{Mn(hfac)_2\}_3(\mathbf{3R})_2$ can be adequately described in the exchange approximation assuming that two magnetic sublattices, one-dimensional ferrimagnetic $\cdots$ –Mn(*1*)–(**3R**)–Mn(*1*)– $\cdots$ chains with four-spin periodicity and Mn(*2*) ions, form a collinear ferrimagnetic structure with a positive exchange coupling. Due to a strong exchange interaction between Mn(*1*) and terminal N–O groups within the chain, it can be considered approximately as a two-spin ferrimagnetic chain made up of middle nitroxide groups ($S = 1/2$) antiferromagnetically coupled with trimer spin species with $S = 3/2$.

The energy of the magnetic anisotropy of $\{Mn(hfac)_2\}_3(\mathbf{3R})_2$ attains 6.2×10^4 erg cm^{-3} at low temperatures and is determined both by the magnetic dipole–dipole interaction and the manganese zero-field level splitting (the single-ion mechanism).

Acknowledgments

This work was supported by a Grant-in-Aid for Scientific Research on Priority Areas (No 09217253) from the Ministry of Education, Science and Culture, Japan, and Nissan Foundation of Science. The authors are greatly indebted to Dr Yuko Hosokoshi for help in the experiments. We also thank the Japan Society for the Promotion of Science for the Special Researcher Fellowship given to ASM.

References

Borrãs-Almenar J J, Burriel R, Coronado E, Gatteschi D and Gõmez-Garsia C J 1991 *Inorg. Chem.* **30** 947
Carlin R L 1986 *Magnetochemistry* (Berlin: Springer)
Coronado E, Drillon M and Georges R 1993 *Research Frontiers in Magnetochemistry* ed C J O'Connor (Singapore: World Scientific) p 27
Coronado E, Drillon M, Nugteren P R, de Longh L J, Beltran D and Georges R 1989 *J. Am. Chem. Soc.* **111** 3874
Drillon M, Coronado E, Beltran D and Georges R 1983 *Chem. Phys.* **79** 449
Franse J J M and Radwanski R 1993 *Handbook on Magnetic Materials* vol 7, ed K H J Buschow (Amsterdam: Elsevier) p 307
Inoue K, Hayamizu T and Iwamura H 1995 *Chem. Lett.* 745
Inoue K, Hayamizu T, Iwamura H, Hashizume D and Ohashi Y 1996 *J. Am. Chem. Soc.* **118** 1803
Inoue K and Iwamura H 1994a *J. Am. Chem. Soc.* **116** 3173
——1994b *J. Chem. Soc., Chem. Commun.* 2274
——1996 *Mol. Cryst. Liq. Cryst.* **286** 133
Ishida T and Iwamura H 1991 *J. Am. Chem. Soc.* **113** 4238
Pei Y, Kahn O J, Sletten J, Renard J P, Georges R, Gianduzzo J C, Curely J and Xu Q 1988 *Inorg. Chem.* **27** 47
Pei Y, Sletten J and Kahn O J 1986a *J. Am. Chem. Soc.* **108** 9143
Pei Y, Verdaguer M, Kahn O J, Sletten J and Renard J P 1986b *J. Am. Chem. Soc.* **108** 7428
——1987 *Inorg. Chem.* **26** 138
Xu Qiang, Darriet J, Soubeyroux J L and Georges R 1988 *J. Magn. Magn. Mater.* **74** 219
Seiden J 1983 *J. Physique Lett.* **44** L947
Sucksmith W and Thompson J E 1954 *Proc. R. Soc.* **225** 362
Verdaguer M, Gleizes A, Renard J P and Seiden J 1984 *Phys. Rev.* B **29** 5144
Walker L R, Dietz R E, Andres K and Darack S 1972 *Solid State Commun*. **11** 593
Wonsowski S W 1971 *Magnetism* (Moscow: Science)